Thermochemical Heat Storage Based on CaO/CaCO3 Cycles

Subjects: Energy & Fuels
Contributor: Yingjie Li

Thermochemical heat storage (TCHS) based on CaO/CaCO3 cycles has broad application prospects due to many advantages, such as high heat storage density, high exothermic temperature, low energy loss, low material price, and good coupling with CSP plants.

Keywords: thermochemical heat storage ; CaO/CaCO3 cycles ; solar energy ; CaO-based material

1. Introduction

In recent years, to deal with global warming and an increasing energy demand, the utilization of renewable resources, such as solar, hydrogen, biofuel, wind energy, and tidal energy, has made strides around the world [1]. Indeed, all countries have reached an agreement to control the temperature rise to 1.5 °C or below [2]. In addition, it has been reported that renewable energy power generation will account for 30% of the total global power generation, surpassing coal-fired power generation for the first time, by 2040 [3]. Nowadays, solar energy is extensively considered to be one of the most promising renewable resources due to its inexhaustibility, safety, and non-pollution. In particular, concentrated solar power (CSP) plants not only have the potential to be integrated into the grid for dispatching power generation [4][5], but have also seen a significant increase in deployment worldwide in recent years [6][7]. However, power production is unstable in the CSP plants due to the intermittent and inconsistent solar energy, which cannot reliably transmit energy to the grid [8][9]. Owing to this, heat storage has become worthy of attention and research that is obligatory, affordable, and efficient [10]. Thermal energy storage (TES) can store heat under sunshine during the day and release heat when there is no solar irradiation. To make solar energy available, it is generally believed that the integration of CSP and TES is a promising and effective option to overcome its limitations [11][12].

There are three forms of TES systems based on different heat storage principles: sensible heat storage (SHS), latent heat storage (LHS), and thermochemical heat storage (TCHS) [13]. SHS takes advantage of the temperature change of the heat storage material to store heat, which is the most mature for industrial applications. The heat storage capacity of SHS depends on the physical properties of the material itself. In addition, SHS materials commonly used in the CSP field mainly include heat transfer oil, molten salts, ceramic, and concrete [14]. LHS is a technology that uses the phase-change process of heat storage materials to store and release heat, so it is also called phase-change heat storage. LHS possesses constant charge/discharge temperature and large heat storage density. Phase change materials (PCMs) mainly include organic, inorganic, and eutectic based on the chemical nature of the materials [15]. However, the traditional PCMs have some problems, such as low thermal conductivity and high energy loss [16]. Thus, the further industrial operation of CSP plants using LHS has been hindered.

In order to improve heat storage efficiency, it is necessary to research and develop new heat storage media with a higher heat storage temperature other than SHS and LHS. Moreover, TCHS absorbs heat through the decomposition of various chemical materials, which store heat energy in the form of chemical energy, and vice versa [17]. TCHS not only achieves a high heat storage density as well as small heat storage volume [12], but can also store energy for a long time at around room temperature [18]. Among the three systems as mentioned above, the special feature of TCHS is that it can store and transmit energy without loss of energy [19]. Therefore, TCHS is considered one of the most promising CSP heat storage technologies [20]. The main characteristics of the abovementioned three heat storage methods are summarized in **Table 1** [21].

Table 1. The main characteristics of the three heat storage methods [19][20][21].

	SHS	LHS	TCHS
Heat storage density	Low ~0.2 GJ/m^3	Medium ~0.3–0.5 GJ/m^3	High ~0.5–3 GJ/m^3
Working temperature	Low	Low or medium	Medium or high
Advantages	Mature technology Low price Long service life	Small heat storage volume Simple system	High heat storage density Small thermal losses Long-distance transportation
Disadvantages	High thermal losses Low heat storage density	Poor thermal conductivity Material corrosion High thermal losses	Complex technology High cost

The different materials used in TCHS systems have been proven feasible, including carbonates [22][23], hydroxides [24][25], metal hydrides [26], metal oxides [27], ammonia [28], methanol [29], and sulfides [30]. Although the current TCHS technology is still immature and remains at the conceptual level, it is becoming an active research field. The common heat storage materials for TCHS are summarized in **Figure 1** [31].

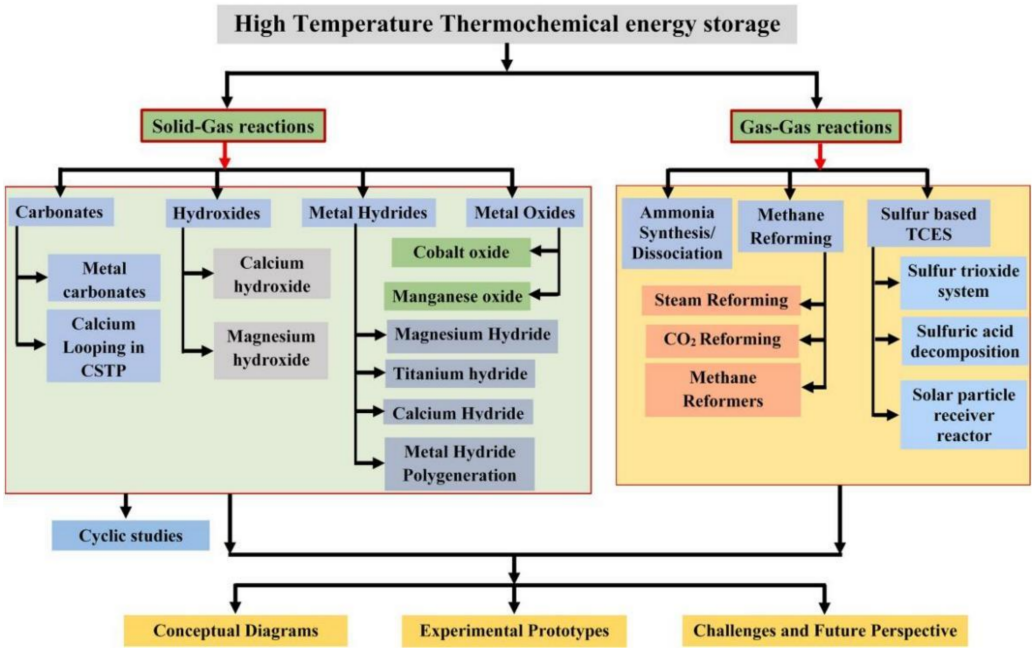

Figure 1. The common heat storage materials for TCHS [31].

Among various TCHS systems, high-temperature thermochemical heat storage based on the carbonation/calcination reaction of CaO/$CaCO_3$ (as exhibited in Equation (1)) is considered to be one of the promising CSP heat storage technologies [32]. CaO/$CaCO_3$ is one of the systems with the highest heat storage density (approximately 3.2 GJ/m^3) [33] and the working temperature is relatively high [34], which is conducive to the realization of large-scale sustainable power generation. The equilibrium temperature of the reaction at atmospheric pressure under pure CO_2 is 895 °C [35]. The reaction equilibrium temperature is determined by the CO_2 partial pressure, as shown in Equation (2) [36].

$$\mathrm{CaCO_3(s) + 178\ kJ/mol \ \leftrightharpoons\ CaCO(s) + CO_2(g)}$$

$$P_{eq} = 4.137 \times 10^7 \exp\left(-\frac{20474}{T}\right)$$

where P_{eq} is the CO_2 partial pressure, bar; T is the equilibrium temperature, K. By changing the CO_2 partial pressure, the carbonator can proceed in the range of 600–900 °C [37]. Additionally, it takes advantage of abundant raw materials and

low prices due to natural calcium-based minerals (limestone or dolomite) as the precursors, which can realize efficient heat storage [38].

2. CaO/$CaCO_3$ TCHS

System design represents a major contribution to the application of CaO/$CaCO_3$ heat storage in CSP plants. The concept of calcium looping (CaL) TCHS can be traced back to the 1970s [39], but most of the subsequent CaL research has focused on CO_2 capture [40]. Only with the increasing demand for heat storage in recent years has the application of CaL in TCHS been extensively studied. Although the CaO/$CaCO_3$ heat storage technology and the CO_2 capture technology have the same chemical reaction principle [41], they have remarkable differences in factors, such as reaction conditions and applications [42]. When the CaL process is utilized for CO_2 capture from the flue gas of coal-fired power plants, the carbonation stage of CaO occurs in a carbonator with the flue gas containing about 15 vol% CO_2 to form $CaCO_3$ at the optimal temperature of 600–700 °C [43][44]. The calcination stage of $CaCO_3$ occurs in a calciner at above 900 °C under a high concentration of CO_2 (>90 vol%) for CO_2 enrichment, where the required heat is provided by fuel oxygen-enriched combustion [45]. When CaL heat storage is implemented in CSP stations, its carbonation and calcination conditions are more flexible. The carbonation reaction is carried out under pure CO_2 for high temperature and power generation efficiency in the exothermic stage. Gases with different concentrations of CO_2 are fed into the carbonator as required, so the exothermic temperature of 600–900 °C can be reached [37]. Increasing the carbonation pressure can improve the limited temperature of the carbonation reaction [46].

In the solar calciner, the reactants generally cannot stay for a long time, so the calcination reaction in the CaO/$CaCO_3$ system needs to be accomplished as soon as possible [32]. Longer reaction time and higher temperature result in more severe sintering of CaO in the calcination stage, which is not beneficial for the carbonation of CaO [47]. Thus, a shorter time and lower temperature lead to a higher carbonation of CaO due to the slight sintering [48][49]. In addition, the solar calciner at low temperature needs fewer solar reflectors, so the cost is also reduced [50][51]. The calcination kinetics depends not only on the calcination temperature, but also on the calcination atmosphere [52]. The different calcination atmospheres for CaO/$CaCO_3$ heat storage were investigated, including CO_2 [52][53], steam [54], and inert gases [49]. For the calcination under pure CO_2 at atmospheric pressure, $CaCO_3$ can only be quickly decomposed at a temperature around 930–950 °C due to the limitation of thermodynamic equilibrium calculated by Equation (2) [49][52]. If the CO_2 partial pressure is higher than the equilibrium pressure, the calcination reaction cannot occur. The utilization of superheated steam (SHS) can reduce the calcination temperature to as low as 680 °C to save energy, and the calcined CaO has strong heat storage activity [54]. Nevertheless, the separation of vapor and CO_2 needs energy consumption. That is because the heat for cooling vapor is difficult to utilize. CO_2 after separation and purification is easier to use and store [55]. The calcination temperature of $CaCO_3$ can be noticeably reduced by using inert gases, such as helium (He) or nitrogen (N_2). Compared with pure N_2, the calcination rate under pure He is faster due to the high diffusivity of CO_2 in He and the high thermal conductivity of He, and the calcination temperature is as low as 725 °C [49]. However, a further issue that needs to be considered is the separation of CO_2 and He. The content related to the reaction conditions will be discussed in detail in the next section. Recently, scholars have conducted lots of research on CaO/$CaCO_3$ heat storage, continuously optimizing the integrated process of CaO/$CaCO_3$ heat storage and CSP power generation to improve efficiency [56][57].

3. Effect of Reaction Conditions on Performance of CaO-Based Materials in CaO/$CaCO_3$ TCHS

For the CaO/$CaCO_3$ TCHS system, whether the CaO-based material can maintain high carbonation performance and cyclic stability are key to heat storage. A number of studies have shown that temperature [58], pressure [59][60], atmosphere [61], and particle size [62] have crucial effects on the sintering rate of CaO-based materials. Therefore, it is necessary to study the reaction conditions in the stages of calcination and carbonation.

The heat storage performances of CaO-based materials are evaluated by the effective conversion [58] and heat storage density [59], respectively. The effective conversion denotes the ratio of the mass of CaO reacted during each carbonation cycle to the total mass of the sample before the carbonation, which is defined by Equation (3):

$$X_{\mathrm{ef},N} = \frac{m_{\mathrm{car},\ N} - m_{\mathrm{cal},\ N-1}}{m_0} \cdot \frac{M_{\mathrm{CaO}}}{M_{\mathrm{CO_2}}}$$

where N denotes the number of TCHS cycles; $X_{\mathrm{ef},\ N}$ is the effective conversion of CaO-based materials after N TCHS cycles; $m_{\mathrm{car},\ N}$ and $m_{\mathrm{cal},\ N-1}$ denote the mass of the sample after the Nth carbonation and the N-1th calcination,

respectively, g; m_0 represents the original mass of the sample, g; M_{CaO} and M_{CO2} represent the molar masses of CaO and CO_2, respectively, g/mol.

Heat storage density represents the maximum heat that can be released per unit mass of CaO-based materials during each carbonation reaction, which is defined by Equation (4):

$$E_{g,\ N} = X_{ef,N} \cdot \frac{1000\Delta H^0}{M_{CaO}}$$

where $E_{g,\ N}$ is the heat storage density of CaO-based materials, kJ/kg; ΔH^0 denotes the standard reaction heat (178 kJ/mol for 0 °C; 165.5 kJ/mol for 900 °C).

4. Performance of CaO-Based Materials in $CaO/CaCO_3$ TCHS

It has been a consensus that the effective conversion of CaO plays a decisive role in the $CaO/CaCO_3$ cycles heat storage. Prieto et al. [63] pointed out that the inactivation of CaO was a major defect for the CSP-CaL system. As the number of $CaO/CaCO_3$ heat storage cycles increases, the activity of CaO decreases rapidly, and usually reaches a lower conversion over 20 cycles [64]. On the one hand, the carbonation occurs rapidly under high CO_2 pressure at high temperature, so the generated $CaCO_3$ layer blocks pores of the unreacted CaO [65]. On the other hand, due to the low Tammann temperature of calcium-based materials, CaO grains are sintered under harsh calcination conditions during multiple $CaO/CaCO_3$ heat storage cycles [47]. The deactivation characteristics of CaO in the heat storage cycles are mainly related to the CaO precursor and the calcination/carbonation conditions. Calcium-based materials include a variety of natural ores, such as limestone, dolomite, and calcium-rich industrial waste such as carbide slag, steel slag, and fly ash [66].

5. Improvement on Cyclic Thermal Storage Stability of CaO-Based Materials in $CaO/CaCO_3$ TCHS

The heat storage performance of natural calcium-based materials, such as limestone and dolomite, declines rapidly with the number of heat storage cycles, which has an adverse effect on the $CaO/CaCO_3$ TCHS. The lower the performance of CaO, the higher the inert solid content of the heat storage system for transportation, preheating, and cooling, resulting in a large amount of energy loss [67]. Studies have shown that the overall efficiency of CSP-CaL power plants increased by more than 10%, as the effective conversion of calcium-based materials increased from 0.07 to 0.5 [68]. Thus, it is beneficial to improve the cyclic heat storage performance of calcium-based materials and prepare calcium-based heat storage materials with high efficiency and stable performance, which have become the focus of attention of researchers. Adding a dopant with a high Tammann temperature to calcium-based materials is one of the most common methods to slow down the sintering of CaO-based materials. The supporter dispersed between the CaO grains plays a supporting role, which prevents the agglomeration of the CaO grains at high temperatures to a certain extent and enhances the sintering resistance of the CaO-based material [69].

6. Improvement on Optical and Thermal Properties of CaO-Based Materials in $CaO/CaCO_3$ TCHS

The Tammann temperature of calcium-based materials is relatively low, so CaO grains agglomerate and grow up during cyclic heat storage process at high temperature, leading to the blockage of the pore structure, which is manifested as a gradual decline in heat storage performance [40][69]. A large number of researches have focused on slowing down the sintering speed of calcium-based heat storage materials to improve cyclic stability. The volumetric heat collection is more suitable for $CaO/CaCO_3$ heat storage system, which requires calcium-based materials with great optical and thermal properties. However, natural calcium-based materials usually have poor optical absorption capacities and thermal conductivity. In recent years, the optical absorption capacity and thermal conductivity of natural calcium-based materials have been given more attention and represent a valuable research direction.

Han et al. [70] prepared composite materials by impregnating in H_3BO_3 solution with $CaCO_3$ and adding expanded graphite with high thermal conductivity for heat storage. They found that the thermal conductivity of the composite materials increased by 60% when 3 wt% expanded graphite was added. The expanded graphite exhibited strong sintering resistance. The heat storage density of the composite material was 1313 kJ/kg after 50 cycles, while that of limestone was only 452 kJ/kg. On this basis, Han et al. [71] also studied an effective compression method to make graphite nanosheets better support the pore structure of CaO-based materials, so the obtained composites possessed a higher volumetric energy density. However, it is worth noting that CO_2 attaches to graphite at high temperatures to form CO gas. More

consideration should be given when choosing graphite as an additive. Da et al. [72] put forward a new idea to increase the blackness of calcium-based materials to achieve the direct absorption of solar energy in a $CaO/CaCO_3$ heat storage system. Their experiments showed that adding black $FeMnO_3$ and Fe_2O_3 to CaO by the sol-gel method improved the optical absorption properties of the materials. When the molar ratio of Ca/Mn/Fe was 100:4:8, the solar absorption of the composite reached 89.81% as exhibited in **Figure 2**. In addition, the existence of $FeMnO_3$ and Fe_2O_3 also enhanced the sintering resistance of CaO. The effective conversion of Ca/Fe/Mn composites remained as high as 0.8 after 20 cycles.

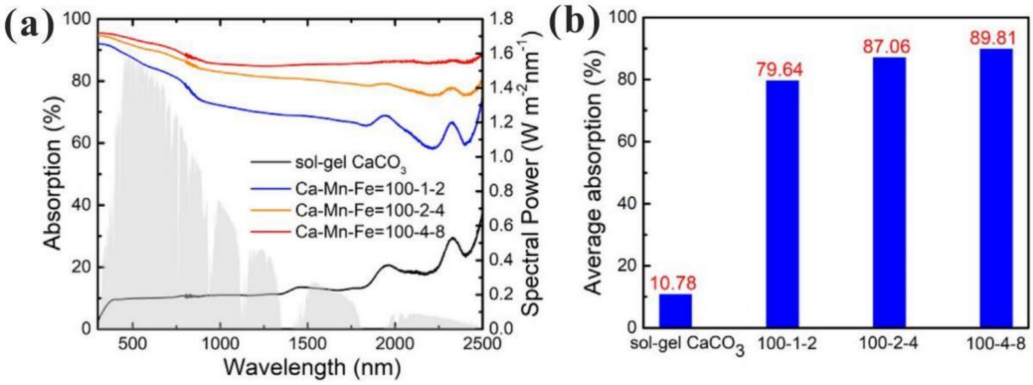

Figure 2. Optical absorption properties of CaO-based composites [72]: (**a**) Spectrum; (**b**) Absorption.

Moreover, Teng et al. [73] optimized the structure of the Ca/Fe/Mn composite by using calcium gluconate as the precursor to prepare a porous Ca/Fe/Mn composite with an optical absorption rate of 90%. The heat storage capacity of the Ca/Fe/Mn composite decreased by 3.31% in 60 cycles. The average heat storage density of the composite after 60 cycles was 1450 kJ/kg, which was 1.76 times as high as that of $CaCO_3$, indicating that it had higher cyclic stability. Song et al. [74] used aluminum nitrate and iron nitrate as precursors to dope iron and aluminum into $CaCO_3$ powder by the sol-gel method. They found that the decomposition rate of the composite increased and the decomposition temperature decreased. After 50 cycles, the heat storage density of the composite only dropped by 4.5%, which was about 87% higher than that of pure $CaCO_3$. Similarly, the average optical absorption rate of the composite achieved 45.6%, while that of pure $CaCO_3$ reached only 8%. Li et al. [75] used $Ca(OH)_2$ powder, $MnC_4H_6O_4{\cdot}4H_2O$ and SiC by extrusion-spheronization method to prepare Mn/SiC doped CaO pellets. They found that when SiC and MnO_2 were both doped at 5 wt%, CaO pellets exhibited the highest the optical absorption and heat storage capacity. In addition, the effective conversion of the Mn/SiC doped CaO pellets remained 0.48 after 30 cycles, while that of the pure CaO pellets achieved only 0.34. Similarly, the average optical absorption of the Mn/SiC doped CaO pellets reached 53%, while that of the original CaO particles was only 3%. Yang et al. [76] prepared Ca/Fe/Mn composite heat storage materials by utilizing carbonaceous microspheres as templates, which mainly consisted of $CaCO_3$ and Ca_2FeMnO_5. The average spectral absorption rate of the synthetic material with the molar ratio of Ca/Fe/Mn = 100:2:7 reached 76.8%, while that of pure $CaCO_3$ was only 10.8%. Zheng et al. [77] examined a variety of dark composite calcium-based heat storage materials by the sol-gel method, including Ca/Cu, Ca/Cu/Fe, Ca/Cu/Co, Ca/Cu/Cr, Ca/Cu/Mn, and Ca/Al/Cu/Fe materials. The results showed that Ca/Cu/Co, Ca/Cu/Cr, and Ca/Cu/Mn materials had strong optical absorption capacities, and their average spectral absorption of solar energy was greater than 60%.

Table 2 summarizes the heat storage properties of the different CaO-based materials reported in the literature. It is found that adding dopants is still the most effective and common method to improve the heat storage stability of CaO-based materials. However, it is still unavoidable that the activity of CaO-based material decreases during long-term heat storage cycles. Calcium-based materials often need to add enough supporters to maintain relatively stable heat storage performance. This also decreases the content of CaO in the calcium-based material, resulting in a decrease in the heat storage density of the material per unit mass. Thus, how to enhance the heat storage performance and cyclic stability of calcium-based materials remain important. In addition, how to improve the optical and thermal properties of CaO-based materials is also the focus of researchers.

Table 2. Comparison of heat storage properties of CaO-based materials reported in the literature.

Additives	Doping Ratio (wt%)	Carbonation Pressure (bar)	Cycles	Effective Conversion	Reference
SiO_2	10%	1	20	0.30	[78]

Additives	Doping Ratio (wt%)	Carbonation Pressure (bar)	Cycles	Effective Conversion	Reference
SiO_2	30%	1	20	0.34	[78]
SiO_2	5%	1	20	0.20	[79]
SiO_2	37.5%	1	45	0.20	[80]
SiO_2	20%	5	50	0.29	[81]
Al_2O_3	20%	5	50	0.62	[81]
Al_2O_3	5%	1	20	0.55	[82]
ZrO_2	5%	1	10	0.22	[83]
ZrO_2	20%	5	50	0.67	[81]
ZrO_2	40%	5	50	0.45	[81]
ZnO	20%	5	50	0.07	[81]
Fe_2O_3	20%	5	50	0.08	[81]
Ni	20%	5	50	0.14	[81]
$BaCO_3$	9.5%	5	50	0.09	[81]
Li_2SO_4	5%	1	11	0.48	[84]
Al_2O_3/CeO_2	5%/5%	13	30	0.79	[85]
Graphite	20%	5	50	0.25	[81]
H_3BO_3/Graphite	3%	1	50	0.41	[70]
Mn/Fe	-	1	20	0.80	[72]
Al/Citric acid	-	1	20	0.7	[86]
Acetic acid(Ac)	-	1	30	0.56	[87]
Mg/Ac	-	1	30	0.70	[87]
NaY	20%	5	50	0.23	[81]
HY	20%	5	50	0.16	[81]

Additives	Doping Ratio (wt%)	Carbonation Pressure (bar)	Cycles	Effective Conversion	Reference
Mor	20%	5	50	0.15	[81]

References

1. Oyekale, J.; Petrollese, M.; Tola, V.; Cau, G. Impacts of Renewable Energy Resources on Effectiveness of Grid-Integrated Systems: Succinct Review of Current Challenges and Potential Solution Strategies. Energies 2020, 13, 4856.
2. Masson-Delmotte, V.; Zhai, P.; Pörtner, H.-O.; Roberts, D.; Skea, J.; Shukla, P.R.; Pirani, A.; Moufouma-Okia, W.; Péan, C.; Pidcock, R. Global Warming of 1.5 °C. An IPCC Special Report on the Impacts of Global Warming; Intergovernmental Panel on Climate Change: Geneva, Switzerland, 2018; Volume 1, pp. 1–9.
3. Dudley, B. BP Energy Outlook. Report–BP Energy Economics; B.P.: London, UK, 2019; Volume 9.
4. Li, J.; Liu, J.; Yan, P.; Li, X.; Zhou, G.; Yu, D. Operation Optimization of Integrated Energy System under a Renewable Energy Dominated Future Scene Considering Both Independence and Benefit: A Review. Energies 2021, 14, 1103.
5. Bravo, R.; Ortiz, C.; Chacartegui, R.; Friedrich, D. Hybrid solar power plant with thermochemical energy storage: A multi-objective operational optimisation. Energy Convers. Manag. 2020, 205, 112421.
6. del Río, P.; Peñasco, C.; Mir-Artigues, P. An overview of drivers and barriers to concentrated solar power in the European Union. Renew. Sustain. Energy Rev. 2018, 81, 1019–1029.
7. Peng, X.; Root, T.W.; Maravelias, C.T. Storing solar energy with chemistry: The role of thermochemical storage in concentrating solar power. Green Chem. 2017, 19, 2427–2438.
8. Ellingwood, K.; Mohammadi, K.; Powell, K. A novel means to flexibly operate a hybrid concentrated solar power plant and improve operation during non-ideal direct normal irradiation conditions. Energy Convers. Manag. 2020, 203, 112275.
9. Ortiz, C.; Binotti, M.; Romano, M.C.; Valverde, J.M.; Chacartegui, R. Off-design model of concentrating solar power plant with thermochemical energy storage based on calcium-looping. AIP Conf. Proc. 2019, 2126, 210006.
10. Heuberger, C.F.; Mac Dowell, N. Real-World Challenges with a Rapid Transition to 100% Renewable Power Systems. Joule 2018, 2, 367–370.
11. Chang, C. Tracking solar collection technologies for solar heating and cooling systems. In Advances in Solar Heating and Cooling; Elsevier: Amsterdam, The Netherlands, 2016; pp. 81–93.
12. Kuravi, S.; Trahan, J.; Goswami, D.Y.; Rahman, M.M.; Stefanakos, E.K. Thermal energy storage technologies and systems for concentrating solar power plants. Prog. Energy Combust. Sci. 2013, 39, 285–319.
13. Pelay, U.; Luo, L.; Fan, Y.; Stitou, D.; Rood, M. Thermal energy storage systems for concentrated solar power plants. Renew. Sustain. Energy Rev. 2017, 79, 82–100.
14. Fernandez, A.I.; Martínez, M.; Segarra, M.; Martorell, I.; Cabeza, L.F. Selection of materials with potential in sensible thermal energy storage. Sol. Energy Mater. Sol. Cells 2010, 94, 1723–1729.
15. Riffat, S.; Mempouo, B.; Fang, W. Phase change material developments: A review. Int. J. Ambient Energy 2015, 36, 102–115.
16. Regin, A.F.; Solanki, S.C.; Saini, J.S. Heat transfer characteristics of thermal energy storage system using PCM capsules: A review. Renew. Sustain. Energy Rev. 2008, 12, 2438–2458.
17. Abedin, A.H.; Rosen, M.A. Closed and open thermochemical energy storage: Energy-and exergy-based comparisons. Energy 2012, 41, 83–92.
18. Wei, L.; Wei, C.; Dandan, W. Research and development of thermochemical energy storage based on hydrated salt. Refrig. Air-Cond. 2017, 17, 14–21.
19. Yan, T.; Wang, R.; Li, T.; Wang, L.; Fred, I.T. A review of promising candidate reactions for chemical heat storage. Renew. Sustain. Energy Rev. 2015, 43, 13–31.
20. Pardo, P.; Deydier, A.; Anxionnaz-Minvielle, Z.; Rougé, S.; Cabassud, M.; Cognet, P. A review on high temperature thermochemical heat energy storage. Renew. Sustain. Energy Rev. 2014, 32, 591–610.
21. Ma, Z.; Wu, S.; Li, Y. Research progress of CO2 capture with the assist CaO-based energy storage materials at coal-fired power station. Clean Coal Technol. 2019, 25, 1–8.

22. Mahon, D.; Claudio, G.; Eames, P. An Experimental Study of the Decomposition and Carbonation of Magnesium Carbonate for Medium Temperature Thermochemical Energy Storage. Energies 2021, 14, 1316.
23. Rhodes, N.R.; Barde, A.; Randhir, K.; Li, L.; Hahn, D.W.; Mei, R.; Klausner, J.F.; AuYeung, N.J. Solar Thermochemical Energy Storage Through Carbonation Cycles of SrCO3/SrO Supported on SrZrO3. ChemSusChem 2015, 8, 3793–3798.
24. Criado, Y.; Alonso, M.; Abanades, J.; Anxionnaz-Minvielle, Z. Conceptual process design of a CaO/Ca(OH)2 thermochemical energy storage system using fluidized bed reactors. Appl. Therm. Eng. 2014, 73, 1087–1094.
25. Seitz, G. Modeling fixed-bed reactors for thermochemical heat storage with the reaction system CaO/Ca(OH)2. Appl. Sci. 2021, 11, 682.
26. Nyallang Nyamsi, S.; Tolj, I.; Lototskyy, M. Metal hydride beds-phase change materials: Dual mode thermal energy storage for medium-high temperature industrial waste heat recovery. Energies 2019, 12, 3949.
27. Preisner, N.C.; Linder, M. A moving bed reactor for thermochemical energy storage based on metal oxides. Energies 2020, 13, 1232.
28. Müller, D.; Knoll, C.; Gravogl, G.; Jordan, C.; Eitenberger, E.; Friedbacher, G.; Artner, W.; Welch, J.M.; Werner, A.; Harasek, M. Medium-temperature thermochemical energy storage with transition metal ammoniates—A systematic material comparison. Appl. Energy 2021, 285, 116470.
29. Li, W.; Hao, Y. Efficient solar power generation combining photovoltaics and mid-/low-temperature methanol thermochemistry. Appl. Energy 2017, 202, 377–385.
30. Wong, B.; Brown, L.; Buckingham, R.; Sweet, W.; Russ, B.; Gorensek, M. Sulfur dioxide disproportionation for sulfur based thermochemical energy storage. Sol. Energy 2015, 118, 134–144.
31. Sunku Prasad, J.; Muthukumar, P.; Desai, F.; Basu, D.N.; Rahman, M.M. A critical review of high-temperature reversible thermochemical energy storage systems. Appl. Energy 2019, 254, 113733.
32. Ortiz, C.; Valverde, J.M.; Chacartegui, R.; Perez-Maqueda, L.A.; Giménez, P. The Calcium-Looping (CaCO3/CaO) process for thermochemical energy storage in Concentrating Solar Power plants. Renew. Sustain. Energy Rev. 2019, 113, 109252.
33. Abedin, A.H.; Rosen, M.A. A critical review of thermochemical energy storage systems. Open Renew. Energy J. 2011, 4, 42–46.
34. Wang, K.; Gu, F.; Clough, P.T.; Zhao, P.; Anthony, E.J. Porous MgO-stabilized CaO-based powders/pellets via a citric acid-based carbon template for thermochemical energy storage in concentrated solar power plants. Chem. Eng. J. 2020, 390, 124163.
35. Barin, I.; Platzki, G. Thermochemical Data of Pure Substances; Wiley Online Library: Hoboken, NJ, USA, 1989; Volume 304.
36. Ortiz, C.; Chacartegui, R.; Valverde, J.; Alovisio, A.; Becerra, J. Power cycles integration in concentrated solar power plants with energy storage based on calcium looping. Energy Convers. Manag. 2017, 149, 815–829.
37. Kyaw, K.; Kubota, M.; Watanabe, F.; Matsuda, H.; Hasatani, M. Study of carbonation of CaO for high temperature thermal energy storage. J. Chem. Eng. Jpn. 1998, 31, 281–284.
38. Cormos, C.-C. Economic evaluations of coal-based combustion and gasification power plants with post-combustion CO2 capture using calcium looping cycle. Energy 2014, 78, 665–673.
39. Wentworth, W.; Chen, E. Simple thermal decomposition reactions for storage of solar thermal energy. Sol. Energy 1976, 18, 205–214.
40. Chen, J.; Duan, L.; Sun, Z. Review on the Development of Sorbents for Calcium Looping. Energy Fuels 2020, 34, 7806–7836.
41. Fedunik-Hofman, L.; Bayon, A.; Donne, S.W. Comparative kinetic analysis of CaCO3/CaO reaction system for energy storage and carbon capture. Appl. Sci. 2019, 9, 4601.
42. Valverde, J.M. The Ca-looping process for CO2 capture and energy storage: Role of nanoparticle technology. J. Nanoparticle Res. 2018, 20, 1–16.
43. Chen, J.; Duan, L.; Sun, Z. Accurate control of cage-like CaO hollow microspheres for enhanced CO2 capture in calcium looping via a template-assisted synthesis approach. Environ. Sci. Technol. 2019, 53, 2249–2259.
44. He, D.; Ou, Z.; Qin, C.; Deng, T.; Yin, J.; Pu, G. Understanding the catalytic acceleration effect of steam on CaCO3 decomposition by density function theory. Chem. Eng. J. 2020, 379, 122348.

45. Martínez, I.; Grasa, G.; Murillo, R.; Arias, B.; Abanades, J. Modelling the continuous calcination of CaCO3 in a Ca-loopi ng system. Chem. Eng. J. 2013, 215, 174–181.

46. Ortiz, C.; Valverde, J.M.; Chacartegui, R.; Perez-Maqueda, L.A. Carbonation of Limestone Derived CaO for Thermoche mical Energy Storage: From Kinetics to Process Integration in Concentrating Solar Plants. ACS Sustain. Chem. Eng. 2 018, 6, 6404–6417.

47. Borgwardt, R.H. Sintering of nascent calcium oxide. Chem. Eng. Sci. 1989, 44, 53–60.

48. Bazaikin, Y.V.; Malkovich, E.; Derevschikov, V.; Lysikov, A.; Okunev, A. Evolution of sorptive and textural properties of C aO-based sorbents during repetitive sorption/regeneration cycles. Chem. Eng. Sci. 2016, 152, 709–716.

49. Sarrion, B.; Valverde, J.M.; Perejon, A.; Perez-Maqueda, L.; Sanchez-Jimenez, P.E. On the Multicycle Activity of Natura l Limestone/Dolomite for Thermochemical Energy Storage of Concentrated Solar Power. Energy Technol. 2016, 4, 101 3–1019.

50. Avila-Marin, A.L. Volumetric receivers in solar thermal power plants with central receiver system technology: A review. Sol. Energy 2011, 85, 891–910.

51. Reich, L.; Melmoth, L.; Yue, L.; Bader, R.; Gresham, R.; Simon, T.; Lipiński, W. A solar reactor design for research on c alcium oxide-based carbon dioxide capture. J. Sol. Energy Eng. 2017, 139, 054501.

52. Valverde, J.M.; Medina, S. Crystallographic transformation of limestone during calcination under CO2. Phys. Chem. Ch em. Phys. 2015, 17, 21912–21926.

53. Charitos, A.; Rodríguez, N.; Hawthorne, C.; Alonso, M.; Zieba, M.; Arias, B.; Kopanakis, G.; Scheffknecht, G.n.; Abanad es, J.C. Experimental validation of the calcium looping CO2 capture process with two circulating fluidized bed carbonat or reactors. Ind. Eng. Chem. Res. 2011, 50, 9685–9695.

54. Arcenegui-Troya, J.; Sánchez-Jiménez, P.E.; Perejón, A.; Moreno, V.; Valverde, J.M.; Pérez-Maqueda, L.A. Kinetics an d cyclability of limestone (CaCO3) in presence of steam during calcination in the CaL scheme for thermochemical ener gy storage. Chem. Eng. J. 2021, 417, 129194.

55. Khosa, A.A.; Xu, T.; Xia, B.Q.; Yan, J.; Zhao, C.Y. Technological challenges and industrial applications of CaCO3/CaO b ased thermal energy storage system—A review. Sol. Energy 2019, 193, 618–636.

56. Lanchi, M.; Turchetti, L.; Sau, S.; Liberatore, R.; Cerbelli, S.; Murmura, M.A.; Annesini, M.C. A Discussion of Possible A pproaches to the Integration of Thermochemical Storage Systems in Concentrating Solar Power Plants. Energies 2020, 13, 4940.

57. Chang, M.-H.; Chen, W.-C.; Huang, C.-M.; Liu, W.-H.; Chou, Y.-C.; Chang, W.-C.; Chen, W.; Cheng, J.-Y.; Huang, K.- E.; Hsu, H.-W. Design and experimental testing of a 1.9 MWth calcium looping pilot plant. Energy Procedia 2014, 63, 2 100–2108.

58. Benitez-Guerrero, M.; Sarrion, B.; Perejon, A.; Sanchez-Jimenez, P.E.; Perez-Maqueda, L.A.; Manuel Valverde, J. Larg e-scale high-temperature solar energy storage using natural minerals. Sol. Energy Mater. Sol. Cells 2017, 168, 14–21.

59. Sun, H.; Li, Y.; Bian, Z.; Yan, X.; Wang, Z.; Liu, W. Thermochemical energy storage performances of Ca-based natural and waste materials under high pressure during CaO/CaCO3 cycles. Energy Convers. Manag. 2019, 197, 111885.

60. Chen, X.; Zhao, N.; Ling, X.; Wang, Y. Parameter analysis of discharging process for CaCO3/CaO thermochemical ene rgy storage. Energy Procedia 2019, 158, 4617–4622.

61. Fedunik-Hofman, L.; Bayon, A.; Hinkley, J.; Lipiński, W.; Donne, S.W. Friedman method kinetic analysis of CaO-based sorbent for high-temperature thermochemical energy storage. Chem. Eng. Sci. 2019, 200, 236–247.

62. Barker, R. The reactivity of calcium oxide towards carbon dioxide and its use for energy storage. J. Appl. Chem. Biotec hnol. 1974, 24, 221–227.

63. Prieto, C.; Cooper, P.; Fernández, A.I.; Cabeza, L.F. Review of technology: Thermochemical energy storage for concent rated solar power plants. Renew. Sustain. Energy Rev. 2016, 60, 909–929.

64. Abanades, J.C. The maximum capture efficiency of CO2 using a carbonation/calcination cycle of CaO/CaCO3. Chem. Eng. J. 2002, 90, 303–306.

65. Valverde, J.M.; Barea-López, M.; Perejón, A.; Sánchez-Jiménez, P.E.; Pérez-Maqueda, L.A. Effect of Thermal Pretreat ment and Nanosilica Addition on Limestone Performance at Calcium-Looping Conditions for Thermochemical Energy S torage of Concentrated Solar Power. Energy Fuels 2017, 31, 4226–4236.

66. Jiang, L. Comprehensiveutnization situation of fly ash in coal-fired power plants and its development suggestions. Clea n Coal Technol. 2020, 26, 31–39.

67. Ortiz, C.; Romano, M.C.; Valverde, J.M.; Binotti, M.; Chacartegui, R. Process integration of Calcium-Looping thermoch emical energy storage system in concentrating solar power plants. Energy 2018, 155, 535–551.

68. Chacartegui, R.; Alovisio, A.; Ortiz, C.; Valverde, J.M.; Verda, V.; Becerra, J.A. Thermochemical energy storage of conc entrated solar power by integration of the calcium looping process and a CO2 power cycle. Appl. Energy 2016, 173, 58 9–605.
69. Scaltsoyiannes, A.A.; Lemonidou, A.A. On the factors affecting the deactivation of limestone under calcium looping con ditions: A new comprehensive model. Chem. Eng. Sci. 2021, 243, 116797.
70. Han, R.; Gao, J.; Wei, S.; Su, Y.; Sun, F.; Zhao, G.; Qin, Y. Strongly coupled calcium carbonate/antioxidative graphite n anosheets composites with high cycling stability for thermochemical energy storage. Appl. Energy 2018, 231, 412–422.
71. Han, R.; Xing, S.; Wu, X.; Pang, C.; Lu, S.; Su, Y.; Liu, Q.; Song, C.; Gao, J. Compressing Two-Dimensional Graphite-N anosheet-Supported CaO for Optimizing Porous Structures toward High-Volumetric-Performance Heat Storage. Energy Fuels 2021, 35, 10841–10849.
72. Da, Y.; Xuan, Y.; Teng, L.; Zhang, K.; Liu, X.; Ding, Y. Calcium-based composites for direct solar-thermal conversion an d thermochemical energy storage. Chem. Eng. J. 2020, 382, 122815.
73. Teng, L.; Xuan, Y.; Da, Y.; Liu, X.; Ding, Y. Modified Ca-Looping materials for directly capturing solar energy and high-te mperature storage. Energy Storage Mater. 2020, 25, 836–845.
74. Song, C.; Liu, X.; Zheng, H.; Bao, C.; Teng, L.; Da, Y.; Jiang, F.; Li, C.; Li, Y.; Xuan, Y.; et al. Decomposition kinetics of A l- and Fe-doped calcium carbonate particles with improved solar absorbance and cycle stability. Chem. Eng. J. 2021, 4 06, 126282.
75. Li, B.; Li, Y.; Dou, Y.; Wang, Y.; Zhao, J.; Wang, T. SiC/Mn co-doped CaO pellets with enhanced optical and thermal pro perties for calcium looping thermochemical heat storage. Chem. Eng. J. 2021, 423, 130305.
76. Yang, L.; Huang, Z.; Huang, G. Fe- and Mn-Doped Ca-Based Materials for Thermochemical Energy Storage Systems. Energy Fuels 2020, 34, 11479–11488.
77. Zheng, H.; Song, C.; Bao, C.; Liu, X.; Xuan, Y.; Li, Y.; Ding, Y. Dark calcium carbonate particles for simultaneous full-sp ectrum solar thermal conversion and large-capacity thermochemical energy storage. Sol. Energy Mater. Sol. Cells 202 0, 207, 110364.
78. Benitez-Guerrero, M.; Valverde, J.M.; Perejon, A.; Sanchez-Jimenez, P.E.; Perez-Maqueda, L.A. Low-cost Ca-based co mposites synthesized by biotemplate method for thermochemical energy storage of concentrated solar power. Appl. En ergy 2018, 210, 108–116.
79. Chen, X.; Jin, X.; Liu, Z.; Ling, X.; Wang, Y. Experimental investigation on the CaO/CaCO3 thermochemical energy stor age with SiO2 doping. Energy 2018, 155, 128–138.
80. Khosa, A.A.; Zhao, C.Y. Heat storage and release performance analysis of CaCO3/CaO thermal energy storage syste m after doping nano silica. Sol. Energy 2019, 188, 619–630.
81. Møller, K.T.; Ibrahim, A.; Buckley, C.E.; Paskevicius, M. Inexpensive thermochemical energy storage utilising additive e nhanced limestone. J. Mater. Chem. A 2020, 8, 9646–9653.
82. Benitez-Guerrero, M.; Valverde, J.M.; Sanchez-Jimenez, P.E.; Perejon, A.; Perez-Maqueda, L.A. Calcium-Looping perf ormance of mechanically modified Al2O3-CaO composites for energy storage and CO2 capture. Chem. Eng. J. 2018, 3 34, 2343–2355.
83. Sarrion, B.; Sanchez-Jimenez, P.E.; Perejon, A.; Perez-Maqueda, L.A.; Valverde, J.M. Pressure Effect on the Multicycle Activity of Natural Carbonates and a Ca/Zr Composite for Energy Storage of Concentrated Solar Power. ACS Sustain. Chem. Eng. 2018, 6, 7849–7858.
84. Lu, S.; Wu, S. Calcination–carbonation durability of nano CaCO3 doped with Li2SO4. Chem. Eng. J. 2016, 294, 22–29.
85. Møller, K.T.; Humphries, T.D.; Berger, A.; Paskevicius, M.; Buckley, C.E. Thermochemical energy storage system devel opment utilising limestone. Chem. Eng. J. Adv. 2021, 8, 100168.
86. Han, R.; Gao, J.; Wei, S.; Su, Y.; Su, C.; Li, J.; Liu, Q.; Qin, Y. High-performance CaO-based composites synthesized u sing a space-confined chemical vapor deposition strategy for thermochemical energy storage. Sol. Energy Mater. Sol. Cells 2020, 206, 110346.
87. Sánchez Jiménez, P.E.; Perejón, A.; Benítez Guerrero, M.; Valverde, J.M.; Ortiz, C.; Pérez Maqueda, L.A. High-perform ance and low-cost macroporous calcium oxide based materials for thermochemical energy storage in concentrated sol ar power plants. Appl. Energy 2019, 235, 543–552.